Piezoelectric allostery of protein

Jun Ohnuki, Takato Sato, and Mitsunori Takano*
Department of Pure and Applied Physics, Waseda University, Tokyo 169-8555, Japan
(Received 10 September 2015; published 13 July 2016)

Allostery is indispensable for a protein to work, where a locally applied stimulus is transmitted to a distant part of the molecule. While the allostery due to chemical stimuli such as ligand binding has long been studied, the growing interest in mechanobiology prompts the study of the mechanically stimulated allostery, the physical mechanism of which has not been established. By molecular dynamics simulation of a motor protein myosin, we found that a locally applied mechanical stimulus induces electrostatic potential change at distant regions, just like the piezoelectricity. This novel allosteric mechanism, "piezoelectric allostery", should be of particularly high value for mechanosensor/transducer proteins.

DOI: 10.1103/PhysRevE.94.012406

A protein molecule is an input-output machine. In the simplest case, it processes a chemical input (substrate), which is bound at a specific (active) site, and releases the products from the active site as the output. In the more elaborate case, an input applied to a specific site of protein is somehow (typically by a large-scale structural change) transmitted to a distant site, altering the structural state of the distant site as the output. The latter I/O property is generally known as "allostery" [1–6]. The initiating input (stimulus) is typically chemical (e.g., ligand binding), and the understanding of the chemically stimulated allostery has been largely advanced by x-ray crystallography that clarifies the difference between ligand-bound and unbound structures [1,3,5].

The allostery is also initiated by a mechanical stimulus [7], which forms the functional basis for the mechanosensor/transducer proteins that are the central players of the recent mechanobiology [8]. However, the molecular mechanism of the mechanically stimulated allostery has not been established, even though molecular dynamics (MD) simulation has begun to demonstrate its potential [9].

Myosin is best known as a molecular motor that drives muscle contraction in concert with actin, and is also a key protein in mechanobiology. Myosin generates mechanical force along the long axis of the actin filament (see Fig. 1) by utilizing the free-energy derived from the hydrolysis of ATP (adenosin triphosphate). Besides this self-generating force, myosin is subjected to external forces (loads) in cellular environment. Supposing that the actin filament, to which myosin binds, is fixed in space, myosin generates or receives those forces at the "lever arm" region. Interestingly, single molecule experiments showed that the load applied to the lever arm alters the affinity of myosin for the ATP-hydrolysis products (ADP and inorganic phosphate) and for the actin filament in a load-direction dependent manner [10–14], which contributes to the efficient unidirectional motion. Since both the ATP-binding and the actin-binding regions are distant from the lever arm region, myosin is thought to be equipped with the mechanically stimulated allostery, although the underlying physical mechanism is unclear.

In this study, to investigate the physical mechanism of the mechanically stimulated allostery, we conducted extensive MD simulation of myosin (long conventional MD simulation reinforced by complementary replica exchange umbrella sampling (REUS) [15]), which enables us to investigate the statistically definite response of myosin as a function of the lever arm position along the actin filament. Since the lever arm position is determined by the position of the base region, called "converter" [16,17] (Fig. 1), and myosin without the lever arm yet with the converter was shown to function normally [18], we truncated the lever arm to reduce the system size and took the position of the center-of-mass of converter as the reaction coordinate. The positive direction of the reaction coordinate, denoted by z, is set to the ATP-driven force direction and the unit is in nanometers throughout this article (therefore omitted).

We first conducted conventional MD simulations starting from the structure with a backward converter position (cyan in Fig. 1) [16] (eight runs, total 1.3 μs) and from the structure with a forward converter position (pink) [17] (eight runs, total 1.0 μs), which resulted in covering a wide range of z. z was adjusted to zero at the most backward position observed during MD, which locates the two starting positions at $z = 2.0$ and 4.8, respectively, and the most forward position during MD at 5.8. By using the structures sampled by the conventional MD simulations that covered the wide range of z ($0 \leqslant z \leqslant 5.8$), we reinforced the sampling by conducting REUS, where the umbrella potential, $K(z - z_0)^2$, was applied to the center-of-mass of the converter, with z_0 shifted from 0 to 5.75 at the intervals of 0.25, resulting in generating 24 replicas. K was set so that the distributions of neighboring replicas substantially overlap each other (42 kJ/mol/nm^2). The exchange of configurations between neighboring replicas was attempted every 100 ps with the acceptance ratio of 34%. The actin binding region [19] was fixed in space by restraint, simulating tight binding of myosin to the actin filament that was not included in the system. Myosin was placed in a truncated octahedron cell, containing 33 000 water molecules [20] and 50 mM KCl, to which the periodic boundary condition was applied. Long-range electrostatic interactions were calculated by PME [21] with the direct space cutoff of 0.8 nm. All simulations were carried out at 310 K and 0.1 MPa using AMBER [22] (with some modification for REUS) and ff03 force-field [23] (these simulation conditions are the same as those employed in the preceding conventional MD simulations). The total run length of REUS was 3.3 μs, and

*Corresponding author: mtkn@waseda.jp

 ©2016 American Physical Society

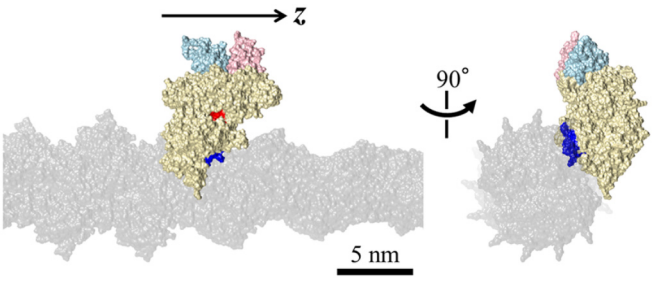

FIG. 1. The structure of scallop myosin II employed in our MD simulation. The converter domain (cyan/pink), to which the lever arm (not shown) is attached, is subjected to the umbrella potential exerted along the long axis (z-axis) of the actin filament (gray). The direction of the ATP-hydrolysis-derived force is to the right, which defines the positive direction of the reaction coordinate z. The backward (cyan) and the forward (pink) converter positions (PDB code 1QVI [16] and 1SR6 [17], respectively) were used as the initial structures of conventional MD simulations. The ATP binding region (red) and the actin binding region [19] (blue) are also indicated.

the snapshot structures saved at 10 ps intervals (total 330 000 snapshot structures) were used for the subsequent electrostatic potential calculations and electrostatic bonds analyses.

We first investigated whether and how the electrostatic potential at the surface of myosin responds to the converter position change, considering that myosin, as well as other proteins, presents characteristic charge distribution due to acidic/basic/polar groups, which plays a crucial role in the electrostatic interaction with actin and associated force generation [24,25]. The electrostatic potential, Φ, was obtained by solving the Poisson-Boltzmann equation for each snapshot structure (total 330 000 snaphots) using APBS [26] (the standard finite difference method was employed with the grid-spacing of 0.3 nm, the interior and exterior dielectric constants of 1 and 78.5, respectively, and the salt concentration of 50 mM). We used the low interior dielectric constant ($\epsilon_{\rm in} = 1$) because the atomic polarization in protein is supposed to be so small that $\epsilon_{\rm in} \sim 1.4$ [27]; note that the dielectric contribution of the dipolar and ionic polarizations is explicitly taken into account in calculating Φ by using the all-atom snapshot structures that were thermally equilibrated. Then the ensemble-averaged Φ, denoted as $\langle\Phi\rangle$, was obtained for each z region with proper reweighting [28] [reweighting had only a little effect on averaging because the z-interval for averaging was small (0.25)]. The ensemble-averaging based on the large number of snapshot structures allowed us to use the relatively large grid-spacing of 0.3 nm (we confirmed that a smaller grid-spacing of 0.1 nm yields the same results within the statistical errors). To remove the translational and rotational movements and possible domain motions of myosin, superimposition onto the reference structure (the average structure for $z = 4.8$) was performed locally (every 10 residue) before averaging.

As shown in Fig. 2(a), it was found that myosin exhibits substantial electrostatic potential change, $\Delta\langle\Phi\rangle$, widespread at the surface when the converter position is moved from the most backward region ($z \in [0,0.25]$) to the most forward region ($z \in [5.5,5.75]$) ($\Delta\langle\Phi\rangle = \langle\Phi\rangle_{z\in[5.5,5.75]} - \langle\Phi\rangle_{z\in[0,0.25]}$). This electrostatic potential change is neither due to the direct

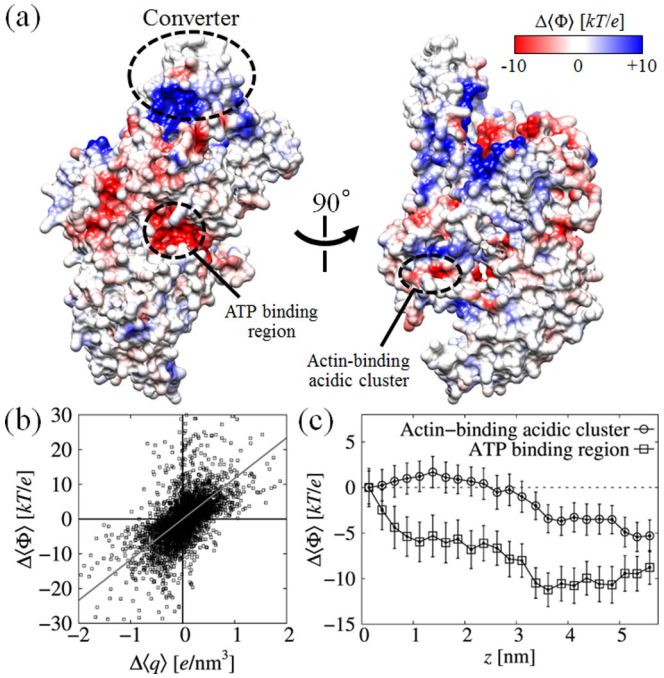

FIG. 2. (a) Electrostatic potential change, $\Delta\langle\Phi\rangle$, at the surface of myosin observed when the converter is moved from the most backward region ($z \in [0,0.25]$) to the most forward region ($z \in [5.5,5.75]$). Potentials are in kT/e ($T = 310$ K). See the color scale bar. $\Delta\langle\Phi\rangle$ was obtained by subtracting $\langle\Phi\rangle$ for the most backward region from that for the most forward region. The direct electrostatic contributions of the converter and surface loops were eliminated. (b) Correlation plot between $\Delta\langle\Phi\rangle$ and the net-charge density change $\Delta\langle q\rangle$. Grid point data (evaluated by trilinear interpolation) covering the entire region of myosin were used for the plot. Correlation coefficient is 0.57. The gray line indicates $\Delta\langle\Phi\rangle = (0.186)^2\Delta\langle q\rangle/2\epsilon_0$, which is expected from the analytical solution of the Poisson equation for the center of a sphere of radius 0.186 nm (volume is 0.027 nm^3) with the charge density $\Delta\langle q\rangle$. (c) $\Delta\langle\Phi\rangle$ for the ATP-binding region (square) and that for the actin-binding acidic cluster (circle) are shown as a function of z ($\langle\Phi\rangle_{[z-0.125,z+0.125]} - \langle\Phi\rangle_{z\in[0,0.25]}$). Standard errors are drawn at 95% confidence interval.

electrostatic influence of the converter, because $\Delta\langle\Phi\rangle$ was calculated so as not to include the direct influence, nor due to domain motions. Therefore $\Delta\langle\Phi\rangle$, exhibiting non-uniform and far-reaching nature, is due to the indirect influence of the converter that propagates inside the protein molecule.

Figure 2(b) shows that the local net-charge density change, $\Delta\langle q\rangle$, correlates well with $\Delta\langle\Phi\rangle$ in myosin encompassing the entire molecule (including both the surface and inner regions). This result indicates that $\Delta\langle\Phi\rangle$ is caused by an extensive alteration of the electric charge distribution $\Delta\langle q\rangle$ that is due to concerted rearrangement of charged groups (detailed analysis is given next). $\Delta\langle\Phi\rangle$ was found to become greater as the converter position is moved forward [Fig. 2(c)]. It is demonstrated that $\Delta\langle\Phi\rangle$s in functionally important two regions, ATP-binding and actin-binding acidic cluster regions [29], become more negative as z is increased. $|e\Delta\langle\Phi\rangle|$ exhibited large values, compared to the thermal energy, in the most forward region ($8.8 \pm 1.9\ kT$ and $5.3 \pm 1.7\ kT$ for the ATP-binding and the actin-binding regions, respectively), and

remained substantial under the condition of $\epsilon_{in} = 2$ and the salt concentration of 100 mM ($4.6 \pm 0.5\ kT$ and $3.5 \pm 0.6\ kT$ for the ATP-binding and the actin-binding regions, respectively). These values of $|e\Delta\langle\Phi\rangle|$ indicate that the movement of the converter possesses a substantial allosteric influence on the binding affinity of charge-carrying molecules (ATP, the hydrolysis products and actin, which were not included in this study). Conversely, the binding of those molecules would exert a substantial allosteric influence on the converter position (discussed later).

We then investigated how the extensive alteration of the charge distribution is induced in the molecule. The charged groups (acidic, basic, and polar groups) usually form electrostatic "bonds" such as ionic and hydrogen bonds inside a protein molecule. An extensive electrostatic bond network is developed in myosin as well. Since the bonds are dynamic in nature, frequently formed and broken and sometimes bifurcated, we calculated the ensemble-averaged number of the electrostatic bonds between amino-acid residues, denoted as $\langle n\rangle$ (note that $\langle n\rangle$ can be more than one). By examining the average bond number change, $\Delta\langle n\rangle$, we found that a large number of electrostatic bonds widespread in the molecule are formed or broken as the converter is moved from the most backward region to the most forward region [Fig. 3(a)]. It is thus demonstrated that $\Delta\langle q\rangle$ is caused by this extensive rearrangement of the electrostatic bond network.

To closely examine the formed/broken bonds and its relationship with $\Delta\langle\Phi\rangle$, we looked into the functionally important two regions mentioned above. For the ATP-binding region [Figs. 3(b) and 3(c)], the negatively charged glutamic acids, Glu177 and Glu465, form electrostatic bonds with Lys182 and Arg242, respectively, in the most backward converter position. As the converter is moved forward, these bonds are weakened, and instead, Glu177 and Glu465 form electrostatic bonds with Arg236, with the Glu177–Arg236 bond stronger than the Glu465–Arg236 bond. In accordance with this bond rearrangement, Glu465 becomes more exposed to the solvent, while Glu177 becomes more buried [the change of solvent accessible surface area was $+10.3(\pm 7.1)$ Å^2 for Glu465 and $-13.8(\pm 5.2)$ Å^2 for Glu177]. Therefore, the negative shift of the electrostatic potential in the ATP-binding region [Fig. 3(c)] is thought to be largely due to the response of Glu465. Note that these basic and acidic residues are highly conserved among species. Particularly, Arg242 and Glu465 are essential residues for the ATP hydolysis reaction [30], and were theoretically identified as key residues that trigger a large-scale structural change [31]. For the actin binding region, Glu534 breaks the electrostatic bonds with the nearby Arg650 [red broken line in Fig. 3(d)] and tends to be isolated [the solvent accessible surface area of Glu534 was increased by $+6.6(\pm 5.5)$ Å^2], which brings about the negative electrostatic potential around Glu534, again consistent with the observed $\Delta\langle\Phi\rangle$. Glu534 constitutes the highly conserved acidic cluster (typically three consecutive acidic residues) that sits in the middle of the actin binding region, and the negative charges in this acidic cluster was shown to strengthen the binding affinity of myosin with actin [29].

Finally, we investigated how the mechanical stimulus due to the converter position propagates though the molecule and reaches distant regions. For this purpose, we analyzed the bond rearrangement network consisting of the formed/broken electrostatic bonds that successively extend from the direct bonds with the converter residues such as Arg710 and Lys759 [31,32] (Fig. 4). It is shown that as the converter is moved forward, the bond rearrangement network gradually grows and reaches the distant regions including the ATP binding and the actin binding regions. This behavior is consistent with the gradual growth of $\Delta\langle\Phi\rangle$ in these regions [Fig. 2(c)] and the retarded growth in the actin binding region which is more distant from the converter. In the bond rearrangement network, alternating succession of formed and broken bonds are frequently observed [as seen in Fig. 3(b)].

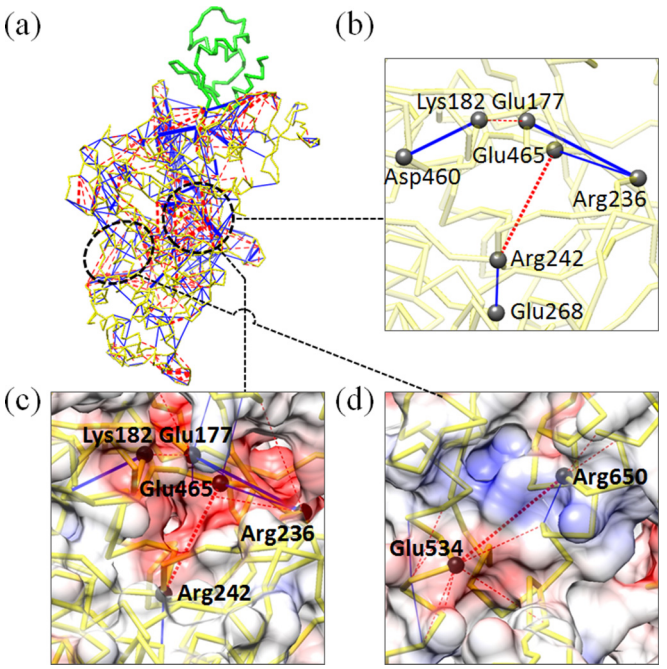

FIG. 3. (a) Rearrangements of electrostatic bonds induced when the converter is moved from the most backward region to the most forward region. An electrostatic bond was judged formed (between acidic, basic, and polar groups) when the distance between H and O (or N, e.g., imino nitrogen in histidine) is less than 0.3 nm. First, the ensemble-averaged number of the electrostatic bonds $\langle n\rangle$ between the bond-forming residues was calculated. Then, the residue pairs that showed substantial change in $\langle n\rangle$ ($|\Delta\langle n\rangle| > \max\{0.1,(\delta n_F^2 + \delta n_B^2)^{1/2}\}$, where δn_F and δn_B are the standard errors of n in the most forward and the most backward regions, respectively) were extracted. Lines are drawn between the extracted residue pairs: red broken lines (total 372 lines) for the pairs with decreased $\langle n\rangle$ and blue solid lines (total 401 lines) for those with increased $\langle n\rangle$ (the larger $|\Delta\langle n\rangle|$, the thicker the line width; the lines involving the converter residues are omitted for clarity, and shown in Fig. 4 instead). Backbone of myosin of the ensemble-averaged structure in the most forward converter position is shown in yellow (the converter in green). (b) Close-up view of the electrostatic bond rearrangement network observed in the ATP binding region. Only the bond rearrangement network involving the key residues are shown. (c) Close-up view with $\Delta\langle\Phi\rangle$ for the ATP binding region and (d) for the acidic cluster in the actin binding region.

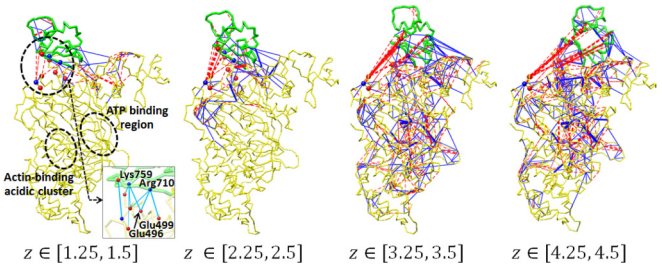

FIG. 4. Propagation of the electrostatic bond rearrangement. Formed/broken electrostatic bonds are extracted and drawn in the same way as in Fig. 3(b) by calculating $\Delta\langle n\rangle$ for the changes from the most backward ensemble ($z \in [0,0.25]$) to the forward ensembles ($z \in [1.25,1.5]$, $z \in [2.25,2.5]$, $z \in [3.25,3.5]$, and $z \in [4.25,4.5]$). Successive bonds that extend from the converter, forming bond rearrangement network, are shown. Inset: bonds (formed for $z \in [0,0.25]$; cyan) involving converter residues are shown. Average backbone structure is rendered for each ensemble.

We thus showed that the positional change of the converter, from which the lever arm extends, induces the polarization charge at the surface and accordingly causes the electrostatic potential change in distant regions. This result implies that if an external force is applied to the lever arm and the converter is forced to move, electrostatic potential change in distant regions is expected to be induced by the applied force. This property is typical of the mechanically stimulated allostery; furthermore, it is characteristic of the piezoelectricity. By combining these two characteristics, we call this property the "piezoelectric allostery".

The piezoelectricity itself is not new to biology but has received little attention even though it can be always expected to arise whenever there is an allostery. One exception is the piezoelectricity in bone [33], which has been intensively studied to reveal the physical mechanism of bone remodeling where bone cells migrate to the region with greater mechanical stress [34]. The bone piezoelectricity is actually due to the constituent protein, collagen [35], but how the collagen molecule responds to the mechanical stimuli is unknown. As for myosin, the piezoelectricity was not reported in the past. However, previous experimental results agree well with the piezoelectricity we found. The retarded dissociation of ADP (ATP hydrolysis product) in the presence of the backward force applied to the lever arm [10–12,14,36] agrees with our observation that the electrostatic potential in the ATP binding region becomes more *positive* as the converter is moved *backward* [Fig. 2(c)]: it is expected that ADP, which is negatively charged, dissociates from the binding site more slowly due to the stronger electrostatic interaction: indeed, by mapping the partial charge distribution of ADP [37] onto the obtained spatial distribution of $\Delta\langle\Phi\rangle$, the electrostatic energy is estimated to be lowered by $\sim 30\,kT$ as the converter is moved backward (note that this energy would be partly offset by the unfavorable electrostatic self-energy, i.e., desolvation energy upon binding [25]). This mechanically stimulated allostery is important for dimeric myosins to walk a long distance on an actin filament [10–12,36].

The stronger binding to actin in the presence of the forward force applied to the lever arm [36] also agrees with our observation that the electrostatic potential at the acidic cluster in the actin binding region becomes more negative as the converter is moved forward [Fig. 2(c)]: negative charge in this cluster was shown to strengthen the actin binding [29]. Furthermore, this piezoelectric allostery is likely to be involved in the force-generation upon strong binding to actin (following the biased Brownian motion during the weak binding) [24,25]: the presence of charges of actin would drive the force-generating forward movement of the converter via the so-called "converse piezoelectric effect". Of course, the electrostatic interaction is weakened as the ionic concentration is increased, but it takes effect substantially for the force generation as long as the salt concentration remains lower than the physiological one ($\sim$100 mM), which we demonstrated in the framework of the Debye-Hückel theory [24,25] (note also that $|\Delta\langle\Phi\rangle|$ remains substantial ($>kT/e$) even at 100 mM as mentioned above). Moreover, the fact that the dielectric constant near the protein surface is lower than that of the bulk water [38,39] should make the piezoelectric effect more conspicuous.

Let us comment on the piezoelectric allostery in a broader context. How an input applied to a certain region of protein is transmitted to a distant site is often explained by sequential and mechanical rearrangements/movements of rigid or semi-rigid elements (e.g., helices and subdomains) [3,40]: in the case of myosin, a seesaw-like mechanical movement of a long rod-like helix was theoretically predicted to transmit the input of the ATP binding region to the converter [31,32]. In contrast, a completely different transmission mechanism due to fluctuation change (without structural change) has recently attracted much attention [4–6]. The piezoelectric allostery is different from these two mechanisms, although some similarities can be recognized in the sequential character [3,40] and in the dispensability of large structural change. Notably, the piezoelectric allostery highlights the electrostatic aspect of allostery, demonstrating the relationship among the mechanical stimulus (input), the electrostatic potential change (output) and the concerted rearrangement of the electrostatic bond network (signal transmission). The rearrangement of the electrostatic bond network was early observed in hemoglobin [3] and recently in kinases [41,42], suggesting its ubiquity in biological functions. The piezoelectric allostery should be of high value for the mechanosensor/transducer proteins that transmit the mechanical input to the downstream proteins that are often regulated electrostatically (e.g., by phosphorylation), and prompts further study of other mechanosensor proteins including collagen [35] and actin [43,44]. Of particular interest is the tension-dependent binding of cofilin (actin depolymerizing protein) [43] and myosin [44] to the actin filament, which is thought to drive the cytoskeleton remodeling and cell motility. The tension-dependent binding may originate from the piezoelectricity of actin. We expect that the piezoelectricity of the actin filament could be quantified by measuring the streaming potential [34] along the actin filament (e.g., oriented actin bundle or sheet) to which mechanical force is applied.

From the viewpoint of the network property, we previously demonstrated that the interaction network within single protein molecules exhibits universal characteristics of a critical percolation cluster [45], which is the case for the electrostatic bond rearrangement network (unpublished data). The criticality may be advantageous for proteins to achieve high responsivity to

the inputs (both chemical and mechanical). In the critically connected network, a limited number of residues would play pivotal roles in achieving the high responsivity. In addition, the highly frustrated nature of the electrostatic network (where favorable and unfavorable interactions coexist) may also be beneficial in preparing a number of metastable states that can be used for regulation. Examining these potential advantages in the cellular environment, where charge perturbations (e.g., addition/removal of a phosphate group) are the most important signals, remains future work.

We thank Koji Umezawa and Taro Uyeda for their valuable comments. This work was supported by Grants-in-Aid for Scientific Research from MEXT (Japan).

[1] B. Alberts, A. Johnson, J. Lewis, M. Raff, K. Roberts, and P. Walter, *Molecular Biology of the Cell*, 5th ed. (Garland Science, New York, 2008).
[2] J. Monod, J. P. Changeux, and F. Jacob, J. Mol. Biol. **6**, 306 (1963).
[3] M. F. Perutz, Nature **228**, 726 (1970).
[4] C. J. Tsai, A. del Sol, and R. Nussinov, Mol. BioSyst. **5**, 207 (2009).
[5] J. P. Changeux, Nat. Rev. Mol. Cell Biol. **14**, 819 (2013).
[6] H. N. Motlagh, J. O. Wrabl, J. Li, and V. J. Hilser, Nature **508**, 331 (2014).
[7] B. Choi, G. Zocchi, Y. Wu, S. Chan, and L. J. Perry, Phys. Rev. Lett. **95**, 078102 (2005).
[8] V. Vogel and M. Sheetz, Nat. Rev. Mol. Cell Biol. **7**, 265 (2006).
[9] M. Sotomayor and K. Schulten, Science **316**, 1144 (2007).
[10] T. J. Purcell, H. L. Sweeney, and J. A. Spudich, Proc. Natl. Acad. Sci. U.S.A. **102**, 13873 (2005).
[11] C. Veigel, S. Schmitz, F. Wang, and J. R. Sellers, Nat. Cell Biol. **7**, 861 (2005).
[12] Y. Oguchi, S. V. Mikhailenko, T. Ohki, A. O. Olivares, E. M. De La Cruz, and S. Ishiwata, Proc. Natl. Acad. Sci. U.S.A. **105**, 7714 (2008).
[13] M. Iwaki, A. H. Iwane, T. Shimokawa, R. Cooke, and T. Yanagida, Nat. Chem. Biol. **5**, 403 (2009).
[14] J. Sung, S. Nag, K. I. Mortensen, C. L. Vestergaard, S. Sutton, K. Ruppel, H. Flyvbjerg, and J. A. Spudich, Nat. Commun. **6**, 7931 (2015).
[15] Y. Sugita, A. Kitao, and Y. Okamoto, J. Chem. Phys. **113**, 6042 (2000).
[16] S. Gourinath, D. M. Himmel, J. H. Brown, L. Reshetnikova, A. G. Szent-Györgyi, and C. Cohen, Structure **11**, 1621 (2003).
[17] D. Risal, S. Gourinath, D. M. Himmel, A. G. Szent-Györgyi, and C. Cohen, Proc. Natl. Acad. Sci. U.S.A. **101**, 8930 (2004).
[18] S. Itakura, H. Yamakawa, Y. Y. Toyoshima, A. Ishijima, T. Kojima, Y. Harada, T. Yanagida, T. Wakabayashi, and K. Sutoh, Biochem. Biophys. Res. Commun. **196**, 1504 (1993).
[19] R. A. Milligan, Proc. Natl. Acad. Sci. U.S.A. **93**, 21 (1996).
[20] W. L. Jorgensen, J. Chandrasekhar, J. D. Madura, R. W. Impey, and M. L. Klein, J. Chem. Phys. **79**, 926 (1983).
[21] T. Darden, D. York, and L. Pedersen, J. Chem. Phys. **98**, 10089 (1993).
[22] D. A. Case *et al.*, *AMBER 9* (University of California, San Francisco, 2006).
[23] Y. Duan *et al.*, J. Comput. Chem. **24**, 1999 (2003).
[24] M. Takano, T. P. Terada, and M. Sasai, Proc. Natl. Acad. Sci. U.S.A. **107**, 7769 (2010).
[25] K. Okazaki, T. Sato, and M. Takano, J. Am. Chem. Soc. **134**, 8918 (2012).
[26] N. A. Baker, D. Sept, S. Joseph, M. J. Holst, and J. A. McCammon, Proc. Natl. Acad. Sci. U.S.A. **98**, 10037 (2001).
[27] A. Warshel and M. Levitt, J. Mol. Biol. **103**, 227 (1976).
[28] S. Kumar, D. Bouzida, R. H. Swendsen, P. A. Kollman, and J. M. Rosenberg, J. Comput. Chem. **13**, 1011 (1992).
[29] M. Furch, B. Remmel, M. A. Geeves, and D. J. Manstein, Biochemistry **39**, 11602 (2000).
[30] N. Sasaki, T. Shimada, and K. Sutoh, J. Biol. Chem. **273**, 20334 (1998).
[31] S. Fischer, B. Windshügel, D. Horak, K. C. Holmes, and J. C. Smith, Proc. Natl. Acad. Sci. U.S.A. **102**, 6873 (2005).
[32] S. Koppole, J. C. Smith, and S. Fischer, Structure **15**, 825 (2007).
[33] E. Fukada and I. Yasuda, J. Phys. Soc. Jpn. **12**, 1158 (1957).
[34] A. C. Ahn and A. J. Grodzinsky, Med. Eng. Phys. **31**, 733 (2009).
[35] C. Halperin, S. Mutchnik, A. Agronin, M. Molotskii, P. Urenski, M. Salai, and G. Rosenman, Nano Lett. **4**, 1253 (2004).
[36] N. Kodera, D. Yamamoto, R. Ishikawa, and T. Ando, Nature **468**, 72 (2010).
[37] K. L. Meagher, L. T. Redman, and H. A. Carlson, J. Comput. Chem. **24**, 1016 (2003).
[38] F. Despa, A. Fernández, and R. S. Berry, Phys. Rev. Lett. **93**, 228104 (2004).
[39] M. Ahmad, W. Gu, T. Geyer, and V. Helms, Nat. Commun. **2**, 261 (2011).
[40] D. E. Koshland, Jr., G. Némethy, and D. Filmer, Biochemistry **5**, 365 (1966).
[41] E. Ozkirimli and C. B. Post, Protein Science **15**, 1051 (2006).
[42] J. Zhou, A. Bronowska, J. Le Coq, D. Lietha, and F. Gräter, Biophys. J. **108**, 698 (2015).
[43] K. Hayakawa, H. Tatsumi, and M. Sokabe, J. Cell Biol. **195**, 721 (2011).
[44] T. Q. P. Uyeda, Y. Iwadate, N. Umeki, A. Nagasaki, and S. Yumura, PLoS ONE **6**, e26200 (2011).
[45] H. Morita and M. Takano, Phys. Rev. E **79**, 020901(R) (2009).